Sliding Mode Control of Two-Wheeled Welding Mobile Robot for Tracking Smooth Curved Welding Path

Tan Lam Chung, Trong Hieu Bui
Department of Mechanical Eng., College of Eng., Pukyong National University, San 100, Yongdang-Dong, Nam-Gu, Pusan 608-739, Korea
Tan Tien Nguyen
Department of Mechanical Eng., Hochiminh City University of Technology, 268 Ly Thuong Kiet, Dist. 10, Hochiminh City, Vietnam
Sang Bong Kim*
Department of Mechanical Eng., College of Eng., Pukyong National University, San 100, Yongdang-Dong, Nam-Gu, Pusan 608-739, Korea

In this paper, a nonlinear controller based on sliding mode control is applied to a two-wheeled Welding Mobile Robot (WMR) to track a smooth curved welding path at a constant velocity of the welding point. The mobile robot is considered in terms of dynamics model in Cartesian coordinates under the presence of external disturbance, and its parameters are exactly known. It is assumed that the disturbance satisfies the matching condition with a known boundary. To obtain the controller, the tracking errors are defined, and the two sliding surfaces are chosen to guarantee that the errors converge to zero asymptotically. Two cases are to be considered : fixed torch and controllable torch. In addition, a simple way of measuring the errors is introduced using two potentiometers. The simulation and experiment on a two-wheeled welding mobile robot are provided to show the effectiveness of the proposed controller.

Key Words : Welding Mobile Robot (WMR), Nonholonomic, Sliding Mode Control

Nomenclature

(x, y) : Coordinates of the WMR's center [m]
ϕ : Heading angle of the WMR [rad]
ν : Linear velocity of the WMR's center [m/s]
ω : Angular velocity of the WMR's center [rad/s]
ω_{rw}, ω_{lw} : Angular velocities of the right and the left wheels [rad/s]
(x_w, y_w) : Coordinates of the welding point [m]
ϕ_w : Heading angle of the welding point [rad]
ν_w : Linear velocity of the welding point [m/s]
ω_w : Angular velocity of the welding point [rad/s]
x_r, y_r : Coordinates of the reference point [m]
ϕ_r : Angle between $\vec{v}$ and x axis [rad]
ν_r : Welding velocity [m/s]
ω_r : Angular velocity of the reference point (the rate of change of $\vec{v}_r$) [rad/s]
b : Distance between driving wheel and the symmetric axis [m]
r : Radius of driving wheel [m]
d : Distance between geometric center and mass center of the WMR [m]
l : Torch length [m]
$M(q)$: Symmetric, positive definite inertia matrix
$V(q, \dot{q})$: Centripetal and coriolis matrix
$B(q)$: Input transformation matrix

* Corresponding Author,
E-mail : memcl@pknu.ac.kr
TEL : +82-51-620-1606; **FAX** : +82-51-621-1411
Department of Mechanical Eng., College of Eng., Pukyong National University, San 100, Yongdang-Dong, Nam-Gu, Pusan 608-739, Korea. (Manuscript **Received** August 26, 2003; **Revised** April 2, 2004)

$A(q)$: Matrix related with the nonholonomic constraints
τ : Control input vector [kgm]
τ_{rw}, τ_{lw} : Torques of the motors which act on the right and the left wheels [kgm]
λ : Constraint force vector
u : Control law which determines error dynamics
m_c : Mass of the body without the driving wheels [kg]
m_w : Mass of each driving wheel with its motor [kg]
I_w : Moment of inertia of each wheel with its motor about the wheel axis [kgm^2]
I_m : Moment of inertia of each wheel with its motor about the wheel diameter [kgm^2]
I_c : Moment of inertia of the body about the vertical axis through the mass center of the WMR [kgm^2]

1. Introduction

Welding automation has been widely used in all types of manufacturing, and one of the most complex applications is welding systems based on autonomous robots. Some special welding robots can provide several benefits in certain welding applications. Among them, welding mobile robot used in line welding application can generates the perfect movements at a certain travel speed, which makes it possible to produce a consistent weld penetration and weld strength.

In practice, some various robotic welding systems have been developed recently. Kim, Ko, Cho and Kim (2000) developed a three dimensional laser vision system for intelligent shipyard welding robot to detect the welding position and to recognize the 3D shape of the welding environments. Jeon, Park and Kim (2002) presented the seam tracking and motion control of two-wheeled welding mobile robot for lattice type welding ; the control is separated into three driving motions : straight locomotion, turning locomotion, and torch slider control. Kam, Jeon and Kim (2001) proposed a control algorithm based on "trial and error" method for straight welding using body positioning sensors and seam tracking sensor. Both of controllers proposed by Jeon and Kam have been successfully applied to the practiced field. Bui, Nguyen, Chung and Kim (2003) proposed a simple nonlinear controller for the two-wheeled welding mobile robot tracking a smooth-curved welding path using Lyapunov function candidate.

On the other hand, there are several works on adaptive and sliding mode control theory for tracking control of mobile robots in literatures, especially, the mobile robots are considered under the model uncertainties and disturbances. Fierro and Lewis (1995) developed a combined kinematics and torque control law using backstepping approach and asymptotic stability is guaranteed by Lyapunov theory which can be applied to the three basic nonholonomic navigation : tracking a reference trajectory, path following and stabilization about a desired posture. Yang and Kim (1999) proposed a new sliding mode control law which is robust against initial condition errors, measurement disturbances and noises in the sensor data to asymptotically stabilize to a desired trajectory by means of the computed-torque method. Fukao, Nakagawa and Adachi (2000) proposed the integration of a kinematic controller and a torque controller for the dynamic model of a nonholonomic mobile robot. In the design, a kinematics adaptive tracking controller is proposed. Then a torque adaptive controller with unknown parameters is derived using the kinematic controller. Chwa, Seo, Kim and Choi (2002) proposed a new sliding mode control method for trajectory tracking of nonholonomic wheeled mobile robots presented in two-dimensional polar coordinates in the presence of the external disturbances ; additionally, the controller showed the better effectiveness in the comparison with the above in terms of the sensitivity to the parameters of sliding surface. Bui, Chung, Nguyen and Kim (2003) proposed adaptive tracking control of two-wheeled welding mobile robot with unknown parameters of moments of inertia in dynamic model.

In this paper, a nonlinear controller using sliding mode control is applied to two-wheeled

welding mobile robot to track a smooth-curved welding path. To design the tracking controller, the errors are defined between the welding point on the torch and the reference point moving at a specified constant welding speed on the welding path. There are two cases of controller: fixed torch controller and controllable torch controller. The two sliding surfaces are chosen to make the errors to approach zeros as reasonable as desired for practical application. The control law is extracted from the stable conditions respectively. The controllable torch controller gives much more performance in comparison with the other. In addition, a simple way for sensing the errors using potentiometers is introduced to realize the above controller. The simulation and experimental studies have been conducted to show the effectiveness of the proposed controller.

2. Dynamic Model of the Welding Mobile Robot

In this section, the dynamic model of a two-wheeled WMR is considered with nonholonomic constraints in relation with its coordinates and the reference welding path.

The WMR is modeled under the following assumptions:

(1) The radius of welding curve is sufficiently larger than turning radius of the WMR.

(2) The robot has two driving wheels for body motion, and those are positioned on an axis passed through the robot geometric center.

(3) Two passive wheels are installed in front and rear of the body at the bottom for balance of mobile platform, and their motion can be ignored in the dynamics.

(4) The velocity at the point contacted with the ground in the plane of the wheel is zero.

(5) The center of mass and the center of rotation of the mobile robot are coincided.

(6) A torch slider is located to coincide the axis through the center of two driving wheels.

(7) A magnet is set up at the bottom of the robot's center to avoid slipping.

The WMR used in this paper is of a two-wheeled mobile robot with some modifications on mechanical structure for welding application as shown in Fig. 1.

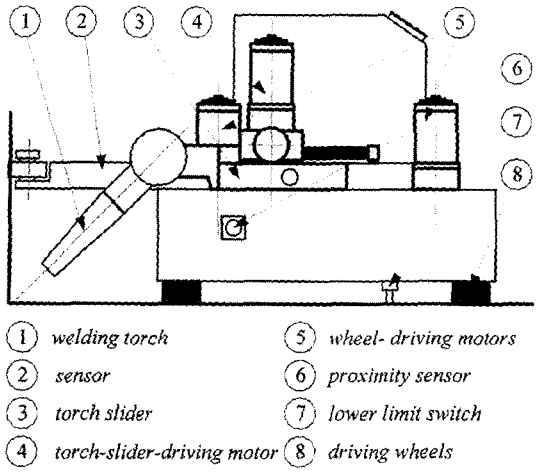

Fig. 1 Configuration of the WMR

The WMR has a geometrical property: the welding point is outside its wheels and is far from the WMR's center. If the torch is fixed, this property leads to the slow convergence of tracking errors. This disadvantage can be overcome by using a controllable torch. As a result, there are three controlled motions in this welding mobile robot: two driving wheels and one torch slider. By including the welding torch motion into the system dynamics, the welding mobile robot can track the reference welding path at welding speed effectively.

The model of two-wheeled welding mobile robot is shown in Fig. 2. The posture of the mobile robot can be described by five generalized coordinates:

$$q=[x\ y\ \phi\ \theta_{rw}\ \theta_{lw}]^T \tag{1}$$

where (x, y) and ϕ are the coordinates and heading angle of the WMR; and θ_{rw} are θ_{lw} the angles of the right and left driving wheels.

Also the internal state variables are chosen as follows:

$$z=[\omega_{rw}\ \omega_{lw}]^T \tag{2}$$

It is assumed that the wheels roll and do not slip, that is, the robot can only move in the direction of the axis of symmetry and the wheels

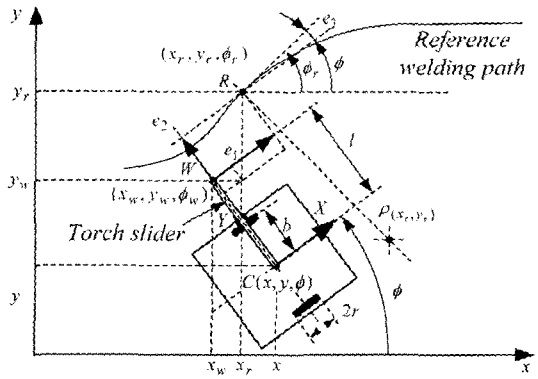

Fig. 2 Two-wheeled WMR model

do not slip. Analytically, the mobile platform satisfies the conditions as following (Fukao, Nakagawa and Adachi, 2000):

$$\begin{cases} \dot{y}\cos\phi-\dot{x}\sin\phi=0 \\ \dot{x}\cos\phi+\dot{y}\sin\phi+b\dot{\phi}=r\omega_{rw} \\ \dot{x}\cos\phi+\dot{y}\sin\phi-b\dot{\phi}=r\omega_{lw} \end{cases} \tag{3}$$

or in the matrix form

$$A(q)\dot{q}=0 \tag{4}$$

where

$$A(q)=\begin{bmatrix} \sin\phi & -\cos\phi & 0 & 0 & 0 \\ \cos\phi & \sin\phi & b & -r & 0 \\ \cos\phi & \sin\phi & -b & 0 & -r \end{bmatrix}$$

The kinematic model under the nonholonomic constraints (4) can be derived as follows:

$$\dot{q}=J(q)z \tag{5}$$

where $J(q)$ is $n\times(n-m)$ a full rank matrix satisfying $J^T(q)A^T(q)=0$.

The system dynamics of the nonholonomic mobile platform in which the constraint Eq. (5) is embedded as follows:

$$\dot{q}=Jz \tag{7}$$

$$J^TMJ\dot{z}+J^T(M\dot{J}+VJ)z=J^TB\tau \tag{8}$$

Multiplying by $(J^TB)^{-1}$, Eq. (8) can be rewritten as follows:

$$\bar{M}(q)\dot{z}+\bar{V}(q,\dot{q})z=\tau \tag{9}$$

where $\bar{M}=(J^TB)^{-1}J^TMJ$,

$$\bar{V}(q,z)=(J^TB)^{-1}J^T(M\dot{J}+VJ)$$

$$q=\begin{bmatrix} x \\ y \\ \phi \\ \theta_{rw} \\ \theta_{lw} \end{bmatrix},\quad J(q)=\begin{bmatrix} \frac{r}{2}\cos\varphi & \frac{r}{2}\cos\varphi \\ \frac{r}{2}\sin\varphi & \frac{r}{2}\sin\varphi \\ \frac{r}{2b} & -\frac{r}{2b} \end{bmatrix},\quad z=\begin{bmatrix} \omega_{rw} \\ \omega_{lw} \end{bmatrix}$$

$$\bar{M}=\begin{bmatrix} \frac{r^2}{4b^2}(mb^2+I)+I_w & \frac{r^2}{4b^2}(mb^2-I) \\ \frac{r^2}{4b^2}(mb^2-I) & \frac{r^2}{4b^2}(mb^2+I)+I_w \end{bmatrix}$$

$$\bar{V}=\begin{bmatrix} 0 & \frac{r^2}{2b}m_cd\dot{\phi} \\ -\frac{r^2}{2b}m_cd\dot{\phi} & 0 \end{bmatrix}$$

$$\tau=\begin{bmatrix} \tau_{rw} \\ \tau_{lw} \end{bmatrix},\quad m=m_c+2m_w,$$

$$I=m_cd^2+2m_wb^2+I_c+2I_m$$

τ_{rw}, τ_{lw} : torques of the motor act on the right and the left wheels

m_c, m_w: mass of the body and wheel with motor

I_c : the moment of inertia of the body about the vertical axis through WMR's center

I_w : the moment of inertia of the wheel with motor about the wheel axis

I_m : the moment of inertia of the wheel with the motor about the wheel diameter

In this paper, the behavior of the welding mobile robot in the presence of external disturbances τ_d is considered. Taking into account the disturbances, real dynamic equation of the welding mobile robot can be derived from Eq. (9) as follows (Yang and Kim, 1999):

$$\bar{M}(q)\dot{z}+\bar{V}(q,\dot{q})z+\tau_d=\tau \tag{10}$$

It is assumed that the disturbance vector can be expressed as a multiplier of matrix $\bar{M}(q)$, or it satisfies the matching condition with a known boundary:

$$\tau_d=\bar{M}(q)f \tag{11}$$

$$f=[f_1, f_2]^T,\ |f_1|\le f_{m_1},\ |f_2|\le f_{m_2} \tag{12}$$

where f_{m_1} and f_{m_2} are upper bounds of disturbances.

The model of the WMR is shown in Fig. 2. It is modeled including the motion of welding torch into system dynamics so that the welding point on torch can track the reference path at specified welding velocity.

First, the kinematic equations of the WMR in the Cartesian space corresponding to Eq. (4) are set up as follows:

$$\begin{bmatrix}\dot{x}\\ \dot{y}\\ \dot{\phi}\end{bmatrix}=\begin{bmatrix}\cos\theta & 0\\ \sin\theta & 0\\ 0 & 1\end{bmatrix}\begin{bmatrix}\nu\\ \omega\end{bmatrix} \tag{13}$$

The relationship between ν, ω and the angular velocities of two driving wheels is given by

$$\begin{bmatrix}\omega_{rw}\\ \omega_{lw}\end{bmatrix}=\begin{bmatrix}1/r & b/r\\ 1/r & -b/r\end{bmatrix}\begin{bmatrix}\nu\\ \omega\end{bmatrix} \tag{14}$$

where ω_{rw} and ω_{lw} represent the angular velocities of the right and left wheels; b is the distance from WMR's center point to the driving wheel; and r is the radius of wheel.

Second, the welding point $W(x_w, y_w)$ on torch and its orientation angle ϕ_w can be derived from the WMR's center $C(x, y)$:

$$\begin{cases}x_w=x-l\sin\phi\\ y_w=y+l\cos\phi\\ \phi_w=\phi\end{cases} \tag{15}$$

where l is the length of torch. The derivative of Eq. (15) yields

$$\begin{bmatrix}\dot{x}_w\\ \dot{y}_w\\ \dot{z}_w\end{bmatrix}=\begin{bmatrix}\cos\phi & -l\cos\phi\\ \sin\phi & -l\sin\phi\\ 0 & 1\end{bmatrix}\begin{bmatrix}\nu\\ \omega\end{bmatrix}+\begin{bmatrix}-\dot{l}\sin\phi\\ \dot{l}\cos\phi\\ 0\end{bmatrix} \tag{16}$$

A reference point $R(x_r, y_r, \phi_r)$ moving with the constant velocity of ν_r on the reference welding path satisfies the following equations:

$$\begin{cases}\dot{x}_r=\nu_r\cos\phi_r\\ \dot{y}_r=\nu_r\sin\phi_r\\ \dot{\phi}_r=\omega_r\end{cases} \tag{17}$$

where ϕ_r is the angle between $\vec{v}_r$ and x coordinate and ω_r is the rate of change of $\vec{v}_r$.

3. Sliding Mode Controller Design

Our objective is to design a controller so that the welding point W tracks the reference point R at a desired constant velocity of welding ν_r. We define the tracking errors $e=[e_1, e_2, e_3]^T$ as shown in Fig. 2:

$$\begin{bmatrix}e_1\\ e_2\\ e_3\end{bmatrix}=\begin{bmatrix}\cos\phi & \sin\phi & 0\\ -\sin\phi & \cos\phi & 0\\ 0 & 0 & 1\end{bmatrix}\begin{bmatrix}x_r-x_w\\ y_r-y_w\\ \phi_r-\phi_w\end{bmatrix} \tag{18}$$

The first derivative of errors yields

$$\begin{bmatrix}\dot{e}_1\\ \dot{e}_2\\ \dot{e}_3\end{bmatrix}=\begin{bmatrix}-1 & e_2+l\\ 0 & -e_1\\ 0 & -1\end{bmatrix}\begin{bmatrix}\nu\\ \omega\end{bmatrix}+\begin{bmatrix}\nu_r\cos e_3\\ \nu_r\sin e_3-\dot{l}\\ \omega_r\end{bmatrix} \tag{19}$$

Also, the second derivative,

$$\begin{bmatrix}\ddot{e}_1\\ \ddot{e}_2\\ \ddot{e}_3\end{bmatrix}=\begin{bmatrix}0 & \dot{e}_2+\dot{l}\\ 0 & -\dot{e}_1\\ 0 & 0\end{bmatrix}\begin{bmatrix}\nu\\ \omega\end{bmatrix}+\begin{bmatrix}-1 & e_2+l\\ 0 & -e_1\\ 0 & -1\end{bmatrix}\begin{bmatrix}\dot{\nu}\\ \dot{\omega}\end{bmatrix}+\begin{bmatrix}-\nu_r\dot{e}_3\sin e_3\\ v_r\dot{e}_3\cos e_3-\ddot{l}\\ \dot{\omega}_r\end{bmatrix} \tag{20}$$

We will design controllers to achieve $e_i\to 0$ as $t\to\infty$; as a result, the welding point W tracks to the reference welding point R at a desired welding velocity.

3.1 The controller for fixed torch

To design the controller for the case of fixed torch ($\dot{l}=0$, $\ddot{l}=0$), the sliding surfaces $s=[s_1\ s_2]^T$ are defined as follows

$$s=\begin{bmatrix}s_1\\ s_2\end{bmatrix}=\begin{bmatrix}\dot{e}_1+k_1e_1+k_2\,\mathrm{sgn}(e_1)|\,e_2\,|\\ \dot{e}_3+k_3e_3\end{bmatrix} \tag{21}$$

where k_1, k_2 and k_3 are positive values and $\mathrm{sgn}(\cdot)$ is the sign function. When reached the sliding surface, the system dynamics satisfies the differential equation obtained from $s=0$, namely,

$$\begin{bmatrix}\dot{e}_1\\ \dot{e}_3\end{bmatrix}=\begin{bmatrix}-k_1e_1-k_2\,\mathrm{sgn}(e_1)|\,e_2\,|\\ -k_3e_3\end{bmatrix} \tag{22}$$

In the first row of (22), when becomes positive, $\dot{e}_1$ becomes negative and vice versa. Thus, the equilibrium point of e_1 converges to zero, which,

in turn, leads to the asymptotic convergence of $|e_2|$ to zero. Similarly, the second row, e_3 also converges to zero.

As a feedback linearization of the system, the control input is defined by computed-torque method as follows (Yang and Kim, 1999)

$$\bar{M}(q)\dot{z}_r+\bar{V}(q,\dot{q})z+\bar{M}(q)u=\tau \tag{23}$$

where $u=[u_1\ u_2]^T$ is a control law which determines error dynamics.

Substitution of the control law (23) into Eq. (10) yields

$$\begin{aligned}&\dot{z}+f=\dot{z}_r+u\\ \Rightarrow\ &\dot{z}-\dot{z}_r=u-f\end{aligned} \tag{24}$$

The following procedure is to design the control law u which stabilizes the sliding surface vector s. From Eqs. (20) and (21) with $\dot{l}=0$ and $\ddot{l}=0$, we have

$$\begin{bmatrix}\dot{e}_1\\ \dot{e}_3\end{bmatrix}=\begin{bmatrix}\dot{e}_2\omega-\dot{\nu}+(e_2+l)\dot{\omega}-\nu_r\dot{e}_3\sin e_3\\ \dot{\omega}_r-\dot{\omega}\end{bmatrix} \tag{25}$$

In this application, the speed of the welding point is constant ($\dot{\nu}_r=0$), Eq. (25) can be rewritten as follows

$$\begin{aligned}\begin{bmatrix}\dot{e}_1\\ \dot{e}_3\end{bmatrix}=&-\begin{bmatrix}(\dot{\nu}-\dot{\nu}_r)\\ (\dot{\omega}-\dot{\omega}_r)\end{bmatrix}\\ &+\begin{bmatrix}\dot{e}_2\omega+(e_2+l)\dot{\omega}-\nu_r\dot{e}_3\sin e_3\\ 0\end{bmatrix}\end{aligned} \tag{26}$$

For the simplicity, Eq. (26) is modified as below

$$\begin{aligned}&\begin{bmatrix}\dot{e}_1+k_1\dot{e}_1+k_2\,\mathrm{sgn}(e_1)|\dot{e}_2|\\ \ddot{e}_3+k_3\dot{e}_3\end{bmatrix}\\ &=-\begin{bmatrix}(\dot{\nu}-\dot{\nu}_r)\\ (\dot{\omega}-\dot{\omega}_r)\end{bmatrix}+\begin{bmatrix}\dot{e}_2\omega+(e_2+l)\dot{\omega}-\nu_r\dot{e}_3\sin e_3\\ 0\end{bmatrix}\\ &+\begin{bmatrix}k_1\dot{e}_1+k_2\,\mathrm{sgn}(e_1)|\dot{e}_2|\\ k_3\dot{e}_3\end{bmatrix}\end{aligned} \tag{27}$$

Substituting Eqs. (21) and (24) into Eq. (27), it reduces to

$$\begin{aligned}\begin{bmatrix}\dot{s}_1\\ \dot{s}_2\end{bmatrix}=&-\begin{bmatrix}u_1\\ u_2\end{bmatrix}+\begin{bmatrix}f_1\\ f_2\end{bmatrix}+\begin{bmatrix}\dot{e}_2\omega+(e_2+l)\dot{\omega}-\nu_r\dot{e}_3\sin e_3\\ 0\end{bmatrix}\\ &+\begin{bmatrix}k_1\dot{e}_1+k_2\,\mathrm{sgn}(e_1)|\dot{e}_2|\\ k_3\dot{e}_3\end{bmatrix}\end{aligned} \tag{28}$$

Let the control law $u=[u_1\ u_2]^T$ be

$$\begin{aligned}\begin{bmatrix}u_1\\ u_2\end{bmatrix}=&\begin{bmatrix}q_1&0\\0&q_2\end{bmatrix}\begin{bmatrix}s_1\\ s_2\end{bmatrix}+\begin{bmatrix}p_1&0\\0&p_2\end{bmatrix}\begin{bmatrix}\mathrm{sgn}(s_1)\\ \mathrm{sgn}(s_2)\end{bmatrix}\\ &+\begin{bmatrix}(\nu_r\sin e_3-e_1\omega)\omega+(e_2+l)\dot{\omega}-\nu_r\dot{e}_3\sin e_3\\ 0\end{bmatrix}\\ &+\begin{bmatrix}k_1\dot{e}_1+k_2\,\mathrm{sgn}(e_1)|\dot{e}_2|\\ k_3\dot{e}_3\end{bmatrix}\end{aligned} \tag{29}$$

where q_i and p_i, $(i=1, 2)$ are positive constant values, then Eq. (28) becomes

$$\dot{s}=-Qs-P\,\mathrm{sgn}(s)+f \tag{30}$$

Define the Lyapunov function as

$$V=\frac{1}{2}s^Ts \tag{31}$$

Its derivative yields

$$\begin{aligned}\dot{V}&=s_1\dot{s}_1+s_2\dot{s}_2=s^T\dot{s}\\ &=s^T(-Qs-P\,\mathrm{sgn}(s)+f)\\ &=-s^TQs-(P|s|-fs)\end{aligned} \tag{32}$$

where,

$$s=\begin{bmatrix}s_1\\ s_2\end{bmatrix};\ Q=\begin{bmatrix}q_1&0\\0&q_2\end{bmatrix};\ P=\begin{bmatrix}p_1&0\\0&f_2\end{bmatrix};\ f=\begin{bmatrix}f_1\\ f_2\end{bmatrix}$$

If we choose $q_i\geq 0$, $p_i\geq f_{m_i}$, $(i=1, 2)$ then $\dot{V}$ turns to be negative semi-definite, and the control law u stabilizes sliding surfaces (21).

3.2 The controller for controllable torch

To design the controller, the sliding surfaces $s=[s_1\ s_2]^T$ are defined as

$$s=\begin{bmatrix}s_1\\ s_2\end{bmatrix}=\begin{bmatrix}\dot{e}_1+k_1e_1\\ \dot{e}_3+k_3e_3\end{bmatrix} \tag{33}$$

Similarly, following the above steps with the new sliding surfaces of Eq. (33), the control law u can be derived as

$$\begin{aligned}\begin{bmatrix}u_1\\ u_2\end{bmatrix}=&\begin{bmatrix}q_1&0\\0&q_2\end{bmatrix}\begin{bmatrix}s_1\\ s_2\end{bmatrix}+\begin{bmatrix}p_1&0\\0&p_2\end{bmatrix}\begin{bmatrix}\mathrm{sgn}(s_1)\\ \mathrm{sgn}(s_2)\end{bmatrix}\\ &+\begin{bmatrix}(\nu_r\sin e_3-e_1\omega+\dot{l})\omega+(e_2+l)\dot{\omega}-\nu_r\dot{e}_3\sin e_3\\ 0\end{bmatrix}\\ &+\begin{bmatrix}k_1\dot{e}_1\\ k_3e_3\end{bmatrix}\end{aligned} \tag{34}$$

We have to design one more controller for torch as follows :

Let the Lyapunov function candidate be

$$V=\frac{1}{2}e_2^2 \tag{35}$$

$$\Rightarrow \dot{V}=e_2\dot{e}_2=e_2(-e_1\omega+v_r\sin e_3-\dot{l}) \tag{36}$$

To achieve $\dot{V}\leq 0$, we choose control law for the torch as follows:

$$\dot{l}=v_r\sin e_3+k_{22}e_2-e_1\omega \tag{37}$$

3.3 Chattering phenomena elimination

In general, chattering must be eliminated for the controller to perform properly. This can be achieved by smoothing out the control discontinuity in a thin boundary layer neighboring the switching surface (Jean-Jacques E. Slotine and Weiping Li, 1991.)

In this case, the welding velocity is rather slow, 7.5 mm/s; consequently, the chattering phenomena makes the motor alternatively change direction, forward and backward by sampling time, to make it impossible to implement the controller. Therefore, a smooth controller is used with a thin boundary layer $\theta=0.1$ instead of the switching controller from Eq. (34) by substituting sign$(\cdot)$ function with sat$(\cdot)$ function, that is,

$$\begin{bmatrix}u_1\\u_2\end{bmatrix}=\begin{bmatrix}q_1&0\\0&q_2\end{bmatrix}\begin{bmatrix}s_1\\s_2\end{bmatrix}+\begin{bmatrix}p_1&0\\0&p_2\end{bmatrix}\begin{bmatrix}\text{sat}\left(\frac{s_1}{\theta}\right)\\\text{sat}\left(\frac{s_2}{\theta}\right)\end{bmatrix}+\begin{bmatrix}(v_r\sin e_3-e_1\omega)\,\omega+(e_2+l)\,\dot{\omega}-v_r\dot{e}_3\sin e_3\\0\end{bmatrix}+\begin{bmatrix}k_1\dot{e}_1\\k_3e_3\end{bmatrix} \tag{38}$$

where the saturation function is defined as

$$\begin{cases}\text{sat}(y)=y & \text{if } |y|\leq 1\\ \text{sat}(y)=\text{sgn}(y) & \text{otherwise}\end{cases} \tag{39}$$

With smoothing approach, the controller (38) can be implemented to the practical welding mobile robot totally. The effectiveness of the controller can be seen through the simulation and the experiment.

3.4 Measurement of the errors

In this paper, the controller is derived from measurement of the tracking errors e_1, e_2, e_3 in Eqs. (29), (34) and (37). The errors measurement scheme is described in Fig. 3: the two rollers are placed at O_1 and O_2 (Bui, Chung, Nguyen and Kim, 2003).

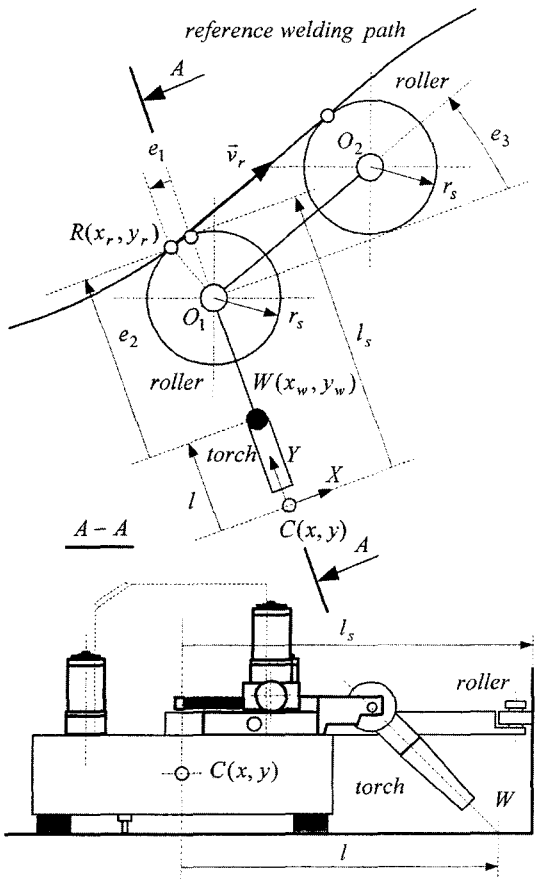

(a)

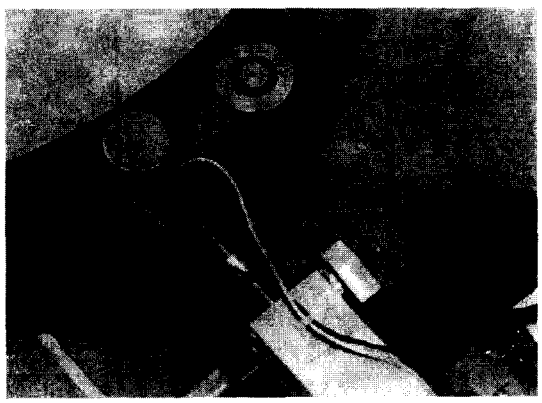

(b)

Fig. 3 Error measurement scheme (a), and its implementation (b)

The roller at O_1 is used to specify the two errors e_1, e_2 and the other, error e_3. The distance between the two rollers O_1O_2 is chosen according to the curve radius of the reference welding path at the contact $R(x_r, y_r)$ such as $\vec{v}_r \,//\, \overrightarrow{O_1O_2}$. The rollers' diameters are chosen small enough to overcome the friction force.

From Fig. 3(a), we have the relationships

$$\begin{cases} e_1 = -r_s \sin e_3 \\ e_2 = (l_s - l) - r_s(1 - \cos e_3) \\ e_3 = \angle(O_1C,\ O_1O_2) - \pi/2 \end{cases} \tag{40}$$

where r_s is the radius of roller, and l_s is the length of sensor. And the two potentiometers are used for measuring the errors: one linear potentiometer for measuring $(l_s - l)$ and one rotating potentiometer, the angular between X coordinate of WMR and $\vec{v}_r$.

4. Simulation and Experimental Results

To verify the effectiveness of the proposed controllers, simulation and experiment have been done for two cases: fixed torch and controlled torch with a reference smooth curved welding path in Fig. 6.

4.1 Hardware of the whole system

The WMR's control system was specially designed for mobile robot with a complicated control law. The control system was modularized on function to perform special control.

The control system is based on the integration of four PIC16F877's: two for servo DC motor controllers, one for servo torch slider controller and one for main controller. The three servo controllers can perform indirect servo control using one encoder. The main controller which is functionalized as master links to the three servo controllers, as slave, via I2C communication. The two A/D ports on master are connected to the two potentiometers for sensing the errors, as mentioned in section 3.4. The total configuration of the control system is shown in Fig. 4.

For operation, the main controller receives signals from sensors to achieve the errors by

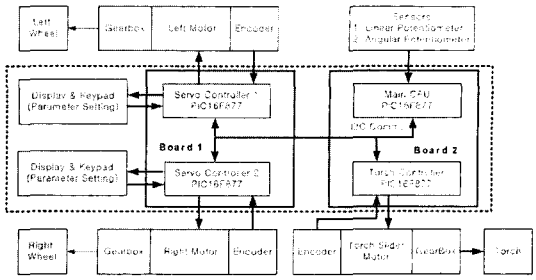

Fig. 4 The configuration of the control system

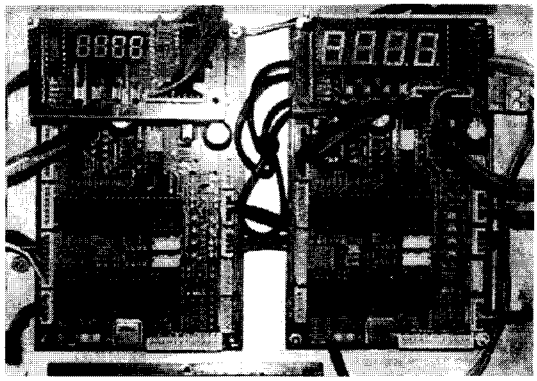

Photo. 1 The controller of the WMR

Eq. (40), then the control laws Eq. (34) are rendered based on the errors for the sampling time of 10 ms, and send the results to the three servo controllers via I2C, respectively.

4.2 Simulation and experimental results

To verify the effectiveness of the proposed controller, simulation has been done for two cases: fixed torch and controllable torch with a defined reference smooth curved welding path (Fig. 5). Also, for the implementation of the practical mobile robot, the simulation for chattering eli mination has been done as well. In addition, the controller was applied to the two-wheeled welding mobile robot for the experiment. It is shown that the welding mobile robot can be used in the practical field.

In the case of fixed torch, the design parameters of the sliding surfaces are $k_1=0.5$, $k_2=0.5$, $k_3=0.7$; and the parameters of the control law $p_1=0.6$, $p_2=2$, $q_1=10$, $q_2=0.35$.

In the case of controllable torch $k_1=1.85$, $k_2=0.8$, $k_3=5$, $k_{22}=2$; $p_1=1$, $p_2=2$; $q_1=10$ and

$q_2=1$. The input disturbances are chosen to be random noises of mean 0 with variance 0.2, and the upper bounds of disturbances are assumed that $f_{m_1}=f_{m_2}=0.5\,N$. The welding speed is 7.5 mm/s. The WMR's parameters and the initial values for the simulation are given in Table 1.

The simulation results are given through Figs. (6) ~ (22). The tracking errors are given in Figs.

Table 1 The numerical values for the simulation

Parameter	Value	Unit	Parameter	Value	Unit
The parameter values of the WMR					
b	0.105	m	d	0.01	m
r	0.025	m	m_c	16.9	kg
m_w	0.3	kg	I_c	0.2081	kgm^2
I_w	3.75×10^{-4}	kgm^2	I_m	4.96×10^{-4}	kgm^2
The initial values of the WMR					
x_r	0.280	m	y_r	0.400	m
x_w	0.270	m	y_w	0.390	m
v	0	mm/s	ω	0	rad/s
ϕ_r	0	deg	ϕ	15	deg
l	0.20	m	ω_r	0	rad/s

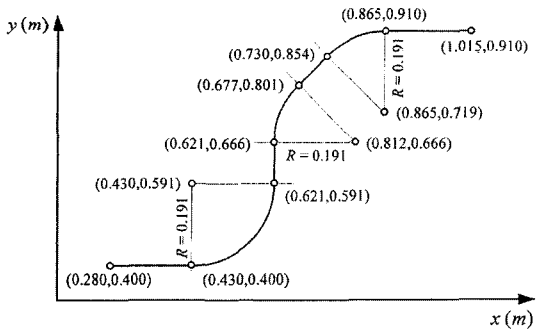

Fig. 5 Smooth curved reference welding path

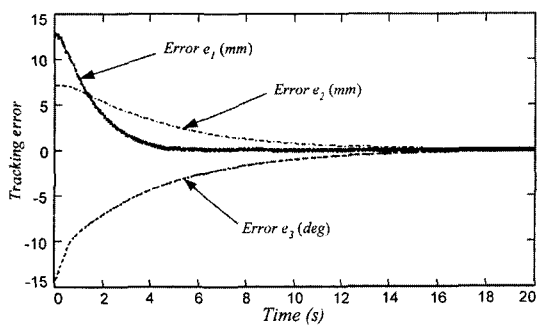

Fig. 6 Tracking errors with fixed torch (20s)

(6) and (7), and it can be seen that the controller with controllable torch, which has the convergent time of 3s, gives much more performance than one with fixed torch, the convergent time of 15s; therefore, from now on, the simulation is presented only for the case of controllable torch.

Figure 8 shows the tracking errors with the chattering phenomena is eliminated. The tracking errors when the mobile robot passes through the

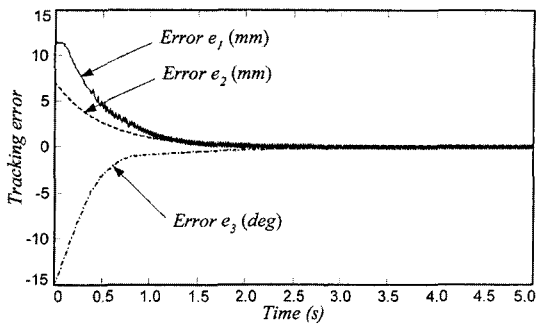

Fig. 7 Tracking errors with controllable torch (5s) without smoothing

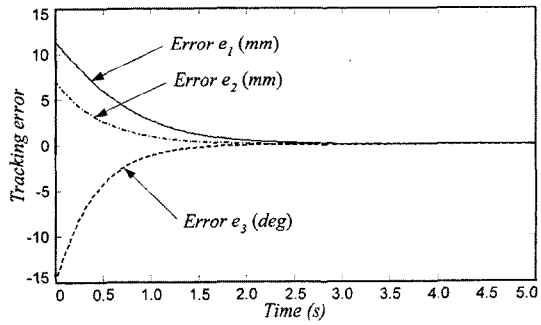

Fig. 8 Tracking errors at beginning (5s) with smoothing

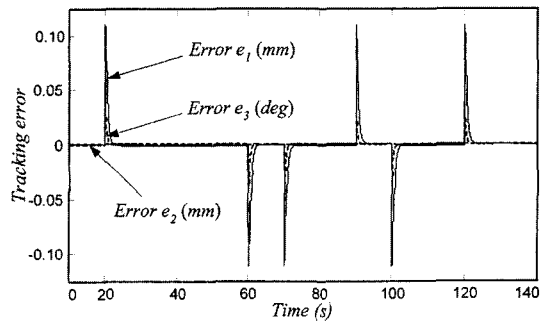

Fig. 9 Tracking errors with smoothing for full time

corner (the joint from straight line to curved line) for full time of 140s are shown in Fig. 9; intuitively, there are quick and sudden changes of errors when the WMR passes through the corners. The sliding surfaces s_1 and s_2 are given in Figs. (10) and (11), respectively.

Figure 12 shows the linear velocity of the WMR; Fig. 13 shows one of the most important parameters: welding velocity. The welding velocity in comparison to linear velocity of the WMR is given in Fig. 14. It can be seen that the welding velocity keeps the welding speed in the vicinity of 7.5 mm/s as desired, even the fluctuation of the WMR's velocity.

The angular velocities of the left and the right wheels without smoothing for the first 5s are

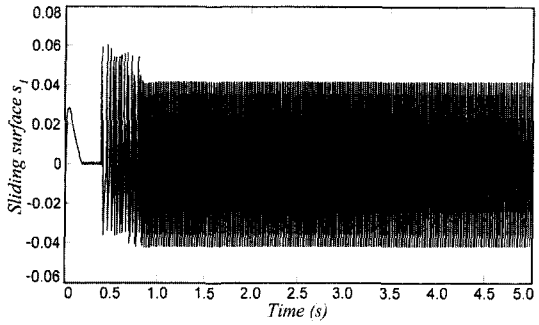

Fig. 10 Sliding surface s_1 at beginning (5s) without smoothing

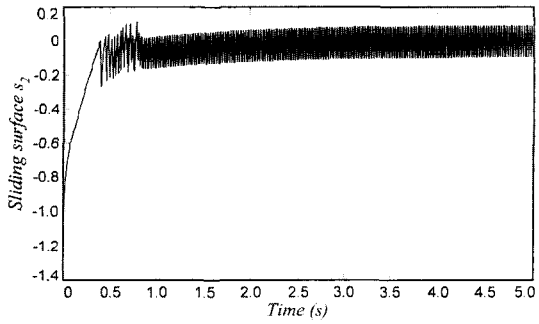

Fig. 11 Sliding surface s_2 at beginning (5s) without smoothing

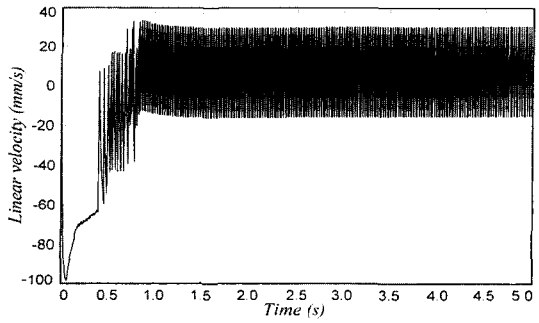

Fig. 12 Linear velocity of the WMR at beginning (5s) without smoothing

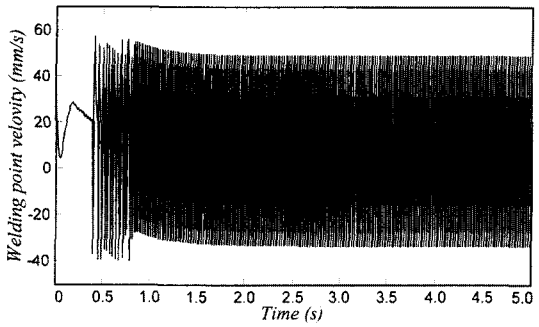

Fig. 13 The welding point velocity at beginning (5s) without smoothing

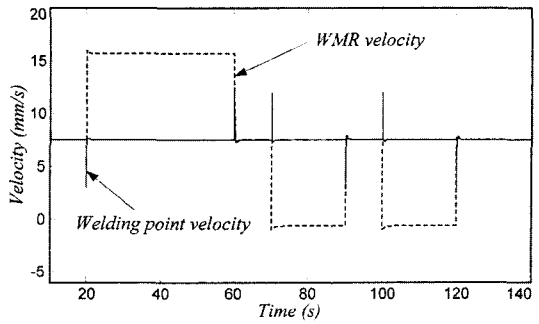

Fig. 14 Linear velocities and welding point with smoothing

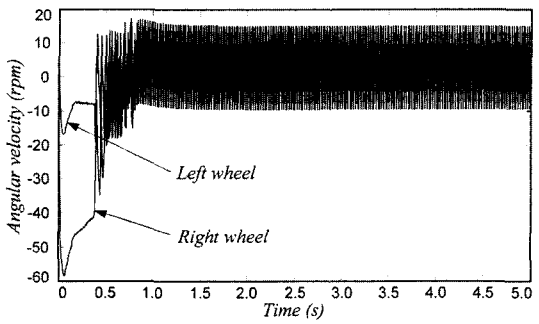

Fig. 15 Angular velocities of two driving wheels at beginning (5s) without smoothing

given in Fig. 15, and we can see that it is impossible to implement the controller because the angular velocities of the two driving wheels are changed direction for a short time (sampling time: 10 ms). Therefore, the chattering elimination is applied to the designed controller as shown in Figs. (16) and (17) for the first 5s and full time of 140s, respectively.

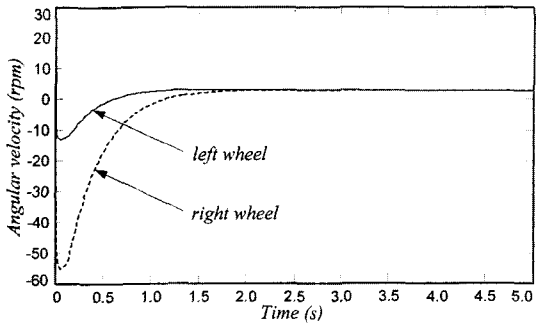

Fig. 16 Angular velocities of two driving wheels at beginning (5s) with smoothing

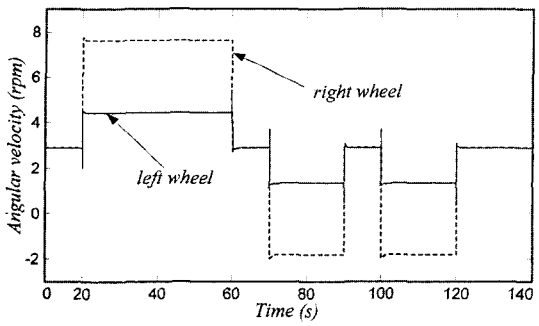

Fig. 17 Angular velocities of two driving wheels with smoothing

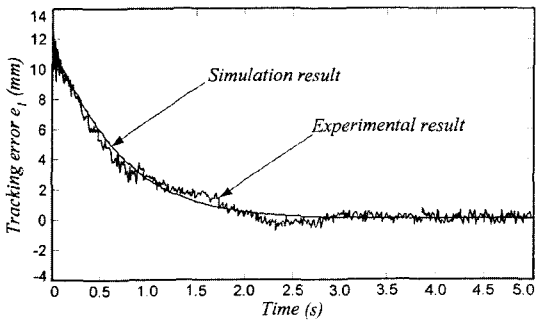

Fig. 18 Experimental tracking errors at beginning (5s)

Additionally, the tracking errors of e_1, e_2 and e_3 of the experiment in the comparison with those of the simulations are shown in Figs. (18) ~ (20), respectively. Also, the controllable torch is used for faster convergence of errors, and its behavior shows the effectiveness of the controllable torch that can compensates for the errors immediately. The torch length is given in Fig. 21. The posture of the welding mobile robot for tracking smooth

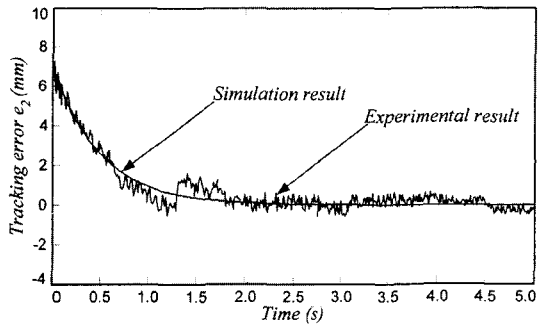

Fig. 19 Experimental tracking errors at beginning (5s)

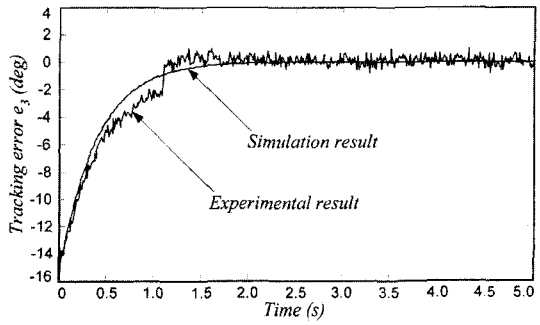

Fig. 20 Experimental tracking errors at beginning (5s)

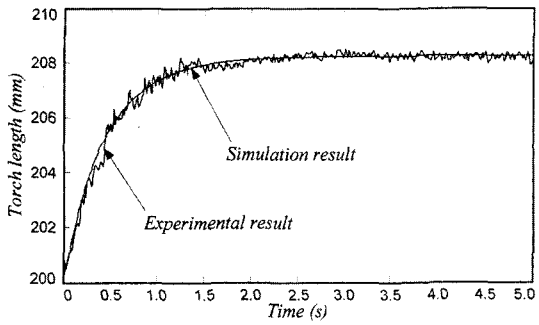

Fig. 21 Experimental torch length at beginning (5s)

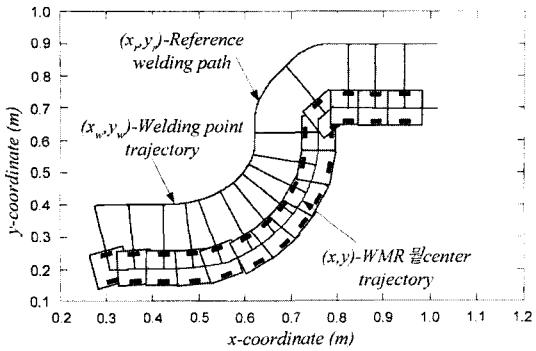

Fig. 22 The tracking movement of the WMR

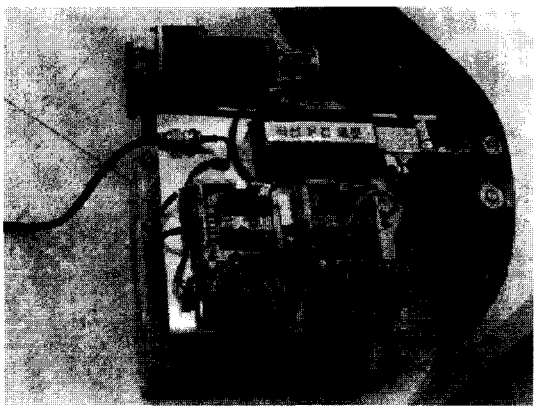

Photo. 2 The experimental WMR

curved welding path is shown in Fig. 22. And the experimental WMR is given in Photo. 2.

From the simulation and experimental results, we can conclude as follows

• The controller for the case of controllable torch gives much more performance in comparison with the other, that is, (i) the time convergence of the errors reduces to 3 seconds ; (ii) the system is less sensitive to the control parameters, if not gentle and flat ; (iii) the convergence of e_2 is fast enough for the welding application.

• The chattering phenomena, as nature of this control, has to be eliminated for the implementation of practical welding mobile robot ; if not, the chattering controller fails to implement for sure.

5. Conclusions

A nonlinear controller based on sliding mode control has been introduced to enhance the tracking performances of the WMR. The controllers were designed in two cases : fixed torch and controllable torch. To design the tracking controllers, an error configuration is defined and the two sliding surfaces are chosen to drive the errors to zero as reasonable as desired. Also, a simple way of measuring the errors for deriving the control law is proposed. Additionally, the chattering elimination has been done for the controller to implement. The simulation and experimental results show that the proposed controller is applicable and can be implemented in the practical field. It can be concluded that the controller with controllable torch gives the much better performance than the other.

References

Bui, T. H., Chung, T. L., Nguyen, T. T. and Kim, S. B., 2003, "Adaptive Tracking Control of Two-Wheeled Welding Mobile Robot with Smooth Curved Welding Path," *KSME International Journal*, Vol. 17, No. 11, pp. 1684~1694.

Bui, T. H., Nguyen, T. T., Chung, T. L. and Kim, S. B., 2003, "A Simple Nonlinear Control of a Two-Wheeled Welding Mobile Robot," *International Journal of Control, Automation, and System (IJCAS)*, Vol. 1, No. 1, pp. 35~42.

Chwa, D. K., Seo J. H., Kim, P. J. and Choi, J. Y., 2002, "Sliding Mode Tracking Control of Nonholonomic Wheeled Mobile Robots," *Proc. of the American Control Conference*, pp. 3991~996.

Fierro, R. and Lewis, F. L., 1997, "Control of a Nonholonomic Mobile Robot : Backstepping Kinematics into Dynamics," *Journal of Robotic Systems*, John Wiley & Sons, Inc., pp. 149~163.

Fukao, T., Nakagawa, H. and Adachi, N., 2000, "Adaptive Tracking Control of a Nonholonomic Mobile Robot," *IEEE Trans. on Robotics and Automation*, Vol. 16, No. 5, pp. 609~615.

Jeon, Y. B., Park, S. S. and Kim, S. B., 2002, "Modeling and Motion Control of Mobile Robot for Lattice Type of Welding," *KSME Inter-*

national Journal, Vol. 16, No. 1, pp. 83~93.

Jean-Jacques E. Slotine and Weiping Li, 1991, *Applied Nonlinear Control*, Prentice-Hall International, Inc., pp. 122~125.

Kam, B. O., Jeon, Y. B. and Kim, S. B., 2001, "Motion Control of Two-Wheeled Welding Mobile Robot with Seam Tracking Sensor," *Proc. IEEE Industrial Electronics*, Vol. 2, pp. 851~856.

Kanayama, Y., Kimura, Y., Miyazaki, F. and Noguchi, T., 1991, "A Stable Tracking Control Method for a Nonholonomic Mobile Robot," *Proc. IEEE Intelligent Robots and Systems Workshop*, Japan, Vol. 3, pp. 1236~1241.

Kim, M. Y., Ko, K. W., Cho, H. S. and Kim, J. H., 2000, "Visual Sensing and Recognition of Welding Environment for Intelligent Shipyard Welding Robots," *Proc. IEEE Intelligent Robots and Systems*, Vol. 3, pp. 2159~2165.

Lee, T. C., Lee, C. H. and Teng, C. C., 1999, "Adaptive Tracking Control of Nonholonomic Mobile Robot by Computed Torque," *Proc. IEEE Decision and Control*, pp. 1254~1259.

Yang, J. M. and Kim, J. H., 1999, "Sliding Mode Control for Trajectory Tracking of Nonholonomic Wheeled Mobile Robots," *IEEE Trans. Robotics and Automation*, Vol. 15, No. 3, pp. 578~587.

Yun, X. and Yamamoto, Y., 1993, "Internal Dynamics of a Wheeled Mobile Robot," *Proc. IEEE Intelligent Robots and Systems*, pp. 1288~1294.